IEEE Access
Multidisciplinary ⋮ Rapid Review ⋮ Open Access Journal

Received 29 October 2023, accepted 11 December 2023, date of publication 18 December 2023,
date of current version 28 December 2023.

Digital Object Identifier 10.1109/ACCESS.2023.3344596

RESEARCH ARTICLE

Partial Discharge Characteristics and Growth Stage Recognition of Electrical Tree in XLPE Insulation

ZHUORAN YANG, YUAN GAO, JINGFANG DENG, AND LIXIANG LV
State Grid Nanjing Power Supply Company, Nanjing 210019, China

Corresponding author: Zhuoran Yang (yangzhuoran@126.com)

This work was supported in part by Technology Project of State Grid Corporation of China (Key Technology Projects of State Grid Jiangsu Electric Power Company Ltd.) under Grant JF2022024.

ABSTRACT Electrical treeing is an inevitable phenomenon during the operation of cross-linked polyethylene (XLPE) cables installed in the underground and humid environment, which is the direct reason for insulation failure. This work focuses on the issue of electrical trees in XLPE insulation and growth stage recognition of treeing stage. The partial discharge (PD) characteristics during different tree growth modes were recorded in the form of φ-q-n patterns. A growth model of electrical trees considering PD process was investigated. The discharge energy was computed, and the relationship between PD characteristics and growth modes of electrical trees was analyzed. A recognition method of the growth stages of electrical trees was given. It was found that PD is mainly distributed in the rising stage of applied voltage, which is the typical characteristic of internal discharge. Tree growth speed depends on the discharge energy that periodically changes during treeing. The increase in PD energy promotes the growth of electrical trees. The growth stage of electrical trees in the rapid growth mode can be recognized by the sparse representation with a recognition accuracy of 90%.

INDEX TERMS Cross-linked polyethylene (XLPE), electrical tree, growth model, partial discharge, PD recognition.

I. INTRODUCTION

Cross-linked polyethylene (XLPE) has been widely used as cable insulation material since the 1860s [1]. Some inevitable defects, such as impurities, protrusions, and cavities, exist in the insulation of XLPE cable, which will induce the electrical trees under the combined effects of electric, thermal, and environmental stresses for a long time. Besides, water trees will be easily formed in the cable insulation in wet conditions, which will be transformed into electrical trees under certain conditions. With the extension of electrical trees, it is easy to form a single-phase ground fault and even lead to power supply system paralysis. Therefore, it is significant to expose the growth of electrical trees to understand the aging mechanism in XLPE and improve the safety and stability of the cable operation.

Partial discharge (PD) is closely related to the growth of electrical trees. Since the discovery of the electrical tree by Kitchin in 1958 [2], many experts and scholars have done a great deal of research work on electrical treeing and their PD characteristics. These researches mainly focus on analyzing a single PD waveform during electrical treeing, the distribution of PD patterns, and the statistical parameters of PD [3], [4], [5], [6], [7], [8], [9]. Yang and Zhang have analyzed the single wave characteristic Weibull distribution parameters of branch-like and bush-like electrical trees under power frequency alternating voltage and proposed that these parameters can distinguish the two kinds of electrical trees [10]. Vogelsang et al. have analyzed the PD patterns and statistical parameters of electrical trees in epoxy resin, and they found that the growth state of electrical trees is closely related to PD [11]. The works of Zheng and Liao show that the PD patterns of electrical trees in XLPE are mostly wing-shaped. PD pattern recognition is suitable for diagnosing electrical trees [12], [13].

The associate editor coordinating the review of this manuscript and approving it for publication was Guillaume Parent.

Although much research has been done on the PD characteristics of different kinds of electrical trees, the relationship between electrical treeing and the characteristics of PD still needs to be determined. Moreover, the PD characteristic in the growth of electrical trees is a basis for completing an online analysis of partial discharge in cable insulation. Therefore, the PD patterns of electrical trees under different growth models were presented in this paper. The experiment was performed under a typical needle-plate electrode. The morphology and PD of the electrical trees were recorded in real time. The change of PD energy under different treeing modes was analyzed. Finally, a growth stage recognition method using sparse representation was introduced.

II. EXPERIMENTAL SETUP

A. SAMPLES AND ELECTRODE

The XLPE insulation block with the size of 20 ×4 ×4 mm used in the experiment was cut from the insulation of commercial XLPE high voltage cable by a microtome. As shown in Figure 1, a typical needle-plane electrode was selected to get an electric field concentration. A steel needle with a diameter of 0.35 mm, a needle tip of 30°, and a curvature radius of 11±3 μm was used to be the high-voltage electrode. A piece of copper foil with a size of 50 mm×50 mm×0.8 mm and a mirror surface was attached as the ground electrode. The distance d between the needle tip and ground electrode was 2±0.2 mm. EVA resin glue was used to fix the sample and ground electrode. Before the test, the samples were observed under a microscope to select the sample without a cavity at the tip of the needle.

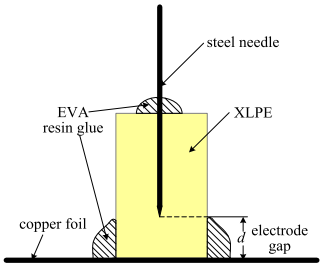

FIGURE 1. Sample and electrode configuration.

It has been found in the previous research [14] that tree initiation voltage in XLPE insulation with an electrode distance of 1∼4 mm is within the range of 7∼8 kVrms at 50 Hz. Therefore, the 50 Hz AC voltage with 8 kVrms was chosen to trigger electrical trees in this paper. In order to improve the reliability of the experimental results, 9 samples with the same electrode spacing of 2±0.2 mm were used to repeat the experiment.

B. EXPERIMENTAL SYSTEM AND PROCEDURES

As shown in Figure 2, the experimental system included five parts: a regulator unit for voltage controlling, XLPE sample, electrodes for electric field concentration, a real-time observation system for treeing data, and a measurement

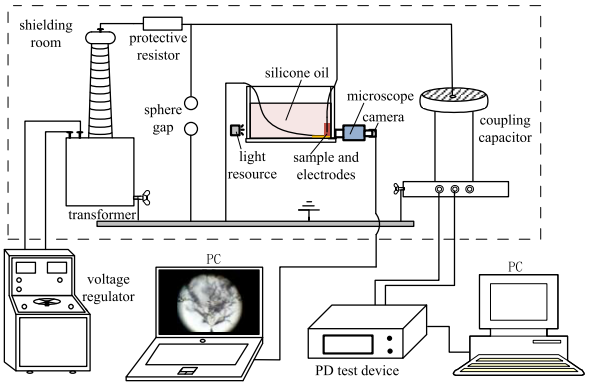

FIGURE 2. Experimental system.

system for PD recording. In the regulator unit, a 100 kV/10 kVA PD-free transformer, a protective resistor, and a pair of sphere gaps were used to protect the transformer from damage when the breakdown occurs. The XLPE sample and needle-plane electrode were fixed in silicone oil to prevent flashover and get clearer structures of electrical trees. The observation system consisting of a cold light source, a CCD a microscope with a magnification of 10 × 5, and a computer was used to record the electrical tree growth process. The PD measurement system consists of a coupling capacitor, a PD detector (HAEFELY DDX9101), and a computer showing the information of PD, such as PRPD patterns (φ-q-n plots, where φ is the phase, q is PD amplitude, and n is the number of PD) at speed of a frame per 5 s. The φ-q-n plots in this paper are PD events for about 300 s. All the experiments were performed at room temperature.

The voltage was risen to 8 kVrms with a rate of 0.5 kV/s. After that, the growth process of electrical trees was recorded, and PD along treeing was measured. The beginning of the electrical tree would be defined as the length of the electrical tree longer than 10 μm if it was recorded by only an optical way. In this experiment, it has been found that PD amplitude was more than 10 pC when the electrical tree grew to 10 μm. As a result, the moment when the PD in the sample was higher than 10 pC has been defined as the beginning of the electrical tree in this work.

III. EXPERIMENTAL RESULTS AND ANALYSIS

A. PD DISTRIBUTION DURING TREEING

The morphological changes of electrical treeing were described in the previous work [14]: the growth modes of electrical trees under the power frequency voltage with an amplitude of 8 kV were categorized into three types, namely, ''breakdown mode,'' ''rapid growth mode'' and ''stagnant growth mode.'' In the breakdown mode, electrical trees grow rapidly after initiation and then break down in a short time. The growth process under rapid growth mode can be divided into four stages. The first stage (stage I) is the initiation stage, during which light-colored electrical trees grow rapidly.

The electrical trees continue to grow at a decreased rate in the second stage (stage II), and the shape of electrical trees gradually changes from branches to pines, the color of the electrical tree deepens, and other short branches begin to grow when the longest branch stops to extend. In the third stage (stage III), electrical trees rapidly develop to the ground electrode. The fourth stage (stage IV) is the sustained growth stage, generating many new branches. However, the insulation between the two electrodes has not been broken down during the test. The stage II and III of ''stagnant growth mode'' are similar to ''rapid growth mode'', except that the duration is longer than that in stage II and stage III of ''stagnant growth mode''.

Figure 3 shows the PD patterns of the breakdown mode. In those patterns, the horizontal axis represents the phase of PD, the vertical axis height represents the amplitude of PD, and the depth of color indicates the number of PD. As shown in Figure 3, PD during initiation distributes in the phase range of $-$ 20°∼135° and 160°∼280°, and the maximum amplitude, Q_{max}, in the positive cycle, is higher than that in the negative cycle, as the internal discharge reported by other researchers [15], [16]. The outline of the PD pattern looks like two mountain peaks. A large number of small amplitude PDs occur at the phase of 35°∼85° and 180°∼250°, and the darker color part in the positive half cycle shows a ''multi-stem'' shape. Combining Figure 3 (a) and (b), it can be concluded that with the increase of applied voltage time, the amplitude and numbers of PDs increase, and the gap of Q_{max} between the positive and negative half cycle decreases. Moreover, the phase distribution of PDs changed little, and the ''multi-stem'' gradually faded away.

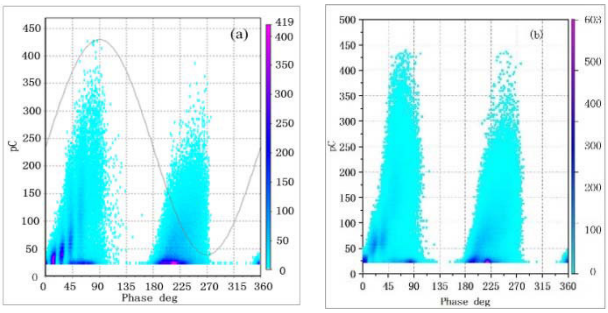

FIGURE 3. φ-q-n plots of PDs due to electrical trees of ''Breakdown Mode'': (a) initiation and (b) propagation.

Figure 4 shows the PD patterns of rapid growth mode. As is seen from Figure 4(a), the PD during initiation occurred in the phase range of −15°∼135° and 159°∼270°, Q_{max} is 248 pC in the positive cycle and 200 pC in the negative cycle. The shape of patterns is similar to that in the breakdown mode. It can be found from Figure 4(b) that, with the increase of applied voltage time, the incipient PD phase shifts right. In the slow growth stage, the amplitude of PDs decreases, and the concentration distribution of PD pattern shifts left. As shown in Figure 4(d), the ''mountain peak'' in the PD pattern of the rapid growth stage is sharper than the others. Moreover, the amplitude of PD rises to the maximum value in the whole

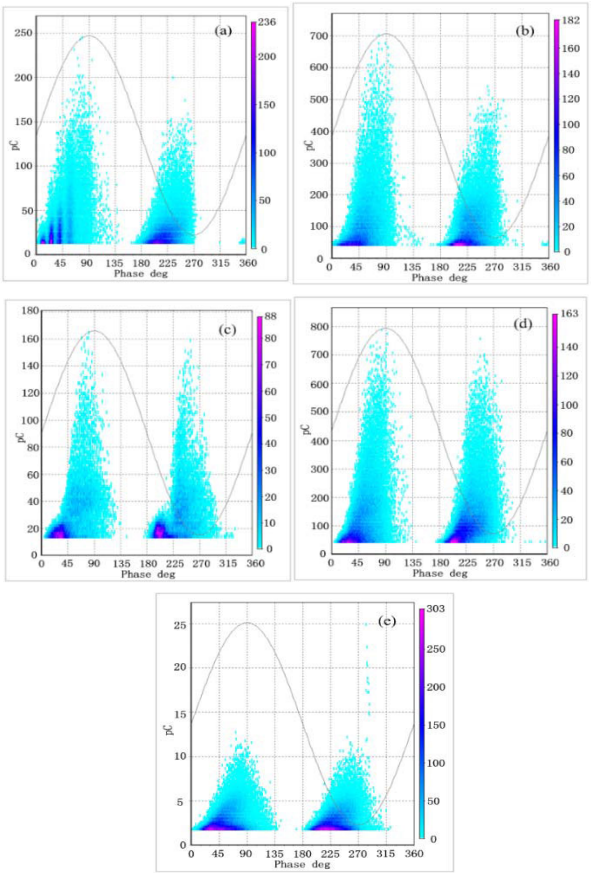

FIGURE 4. φ-q-n plots of PDs due to electrical trees of ''Rapid Growth Mode'': (a) and(b) initiation, (c) the slow growth stage, (d) the rapid growth stage, and (e) the sustained growth stage.

growth process, and the PD patterns of two half cycles are almost symmetrical. In stage II, small-magnitude PDs also occur, as shown in Figure 4(e). Therefore, the discharge energy is very small, and it is not enough to push the PDs to reach the tip of the branches. Then, the insulation at the front of the branches fails to break down.

The PD patterns of stagnant growth mode are shown in Figure 5. It can be observed that PDs are distributed over the whole phase cycle except the range of 280°∼310°. The PD patterns of two half cycles are almost symmetrical. The Q_{max} is 140 pC, and the darker color part in the two half cycles shows a ''diagonal strip'' shape, as shown in Figure 5(a). As shown in Figure 5(b), with the increase of the applied voltage, the dark ''diagonal strip'' gradually disappears, and the distribution of PDs shifts right. Besides, PD magnitude increases gradually, and the difference in PD level between the positive and negative half cycle becomes larger. Figure 5(c) shows the PD pattern of the electrical trees at its rapid growth stage. The outline of this pattern is a trapezoid shape, and the darker color part shows a ''bubble'' shape. Although the magnitude of the ''bubble-like'' PD pattern is small, its number is large. As shown in Figure 5(d), the PD pattern of electrical trees at the sustained growth stage is a hilly shape with a smaller amplitude.

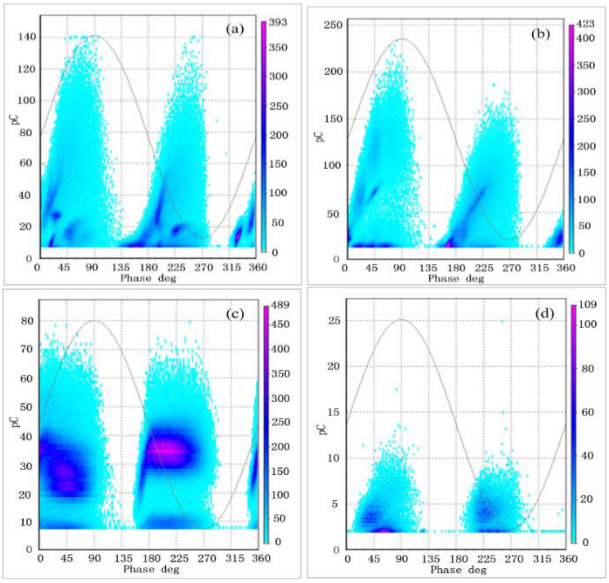

FIGURE 5. φ-q-n plots of PDs due to electrical trees of "Stagnant Growth Mode": (a) initiation, (b) the slow growth stage, (c) the rapid growth stage, and (d) the sustained growth stage.

The experimental results show that the outline of PD patterns during treeing almost looks like a ''mountain peak''. And most of the PDs distributed at the rising part of sinusoidal voltage, showing the characteristics of typical internal discharge. The deep-colored ''multi-stem'' shape occurs in the positive half cycle of PD patterns during the initiation stage in all growth modes, which will disappear with the increased applied voltage time. As for the amplitude of PDs during initiation, the value in breakdown mode is maximum, followed by rapid growth mode, and the minimum value is in stagnant growth mode. While only small magnitude PDs exist in the sustained growth stage of fast growth mode and stagnant growth mode. Moreover, a small magnitude PD concentration area can be found in all the PD patterns.

B. PD MECHANISM OF ELECTRICAL TREEING

The maximum electric field, E_{max}, in front of the needle tip under AC voltage, can be calculated by the Mason formula [17],

$$E_{\max} = \frac{2U_p}{r \ln(1 + \frac{4d}{r})} \tag{1}$$

where U_P is the peak voltage, r is the curvature radius of the needle tip, and d is the distance between two electrodes.

According to the Mason formula, when the applied voltage reached 8 kVrms, the maximum electric field intensity existed in front of the top of the needle tip is 317 kV/mm, which exceeds the critical electric field value (285 kV/mm [18]) of the space charge injection in XLPE. Thus, charges are injected into the insulation in front of the needle tip after applying voltage. Besides, a cavity forms in front of the needle tip before electrical trees are initiated [19]. When the applied voltage instantaneous value rises to the PD inception voltage (PDIV) value of the air gap, PD occurs, and gas molecules are ionized, resulting in a large number of space charges that move to the channel wall under the effect of electric field, as shown in Figure 6(a). Afterward, the electric field, $\vec{E}$, in the discharge channel can be expressed by:

$$\vec{E} = \vec{E}_0 + \vec{E}_q \tag{2}$$

where $\vec{E}_0$ is the electric field formed by the applied voltage, and $\vec{E}q$ is the electric field formed by space charges.

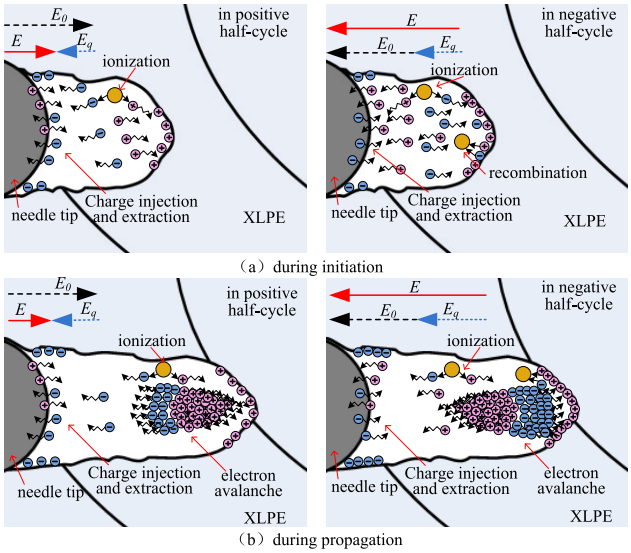

FIGURE 6. PD process of treeing.

In the positive half cycle of sinusoidal voltage, the increase of instantaneous voltage induces PD. Thus, PDs of electrical treeing are mainly distributed at the range of 0°∼90° and 180°∼270°. In addition, the magnitude of PDs increases with the rise of instantaneous voltage. Therefore, PD patterns show a ''bimodal shape''. However, when the applied voltage drops to a certain value in the decline part of the positive half cycle, E_q would be greater than E_0, and the deviation (E_q - E_0) exceeded the air gap breakdown field, negative discharge would occur, as shown in t_3 point of Figure 7. The negative discharge also appears in the decline part of the negative half cycle, as shown in Figure 7, point t_5, whose formation mechanism is similar to that in the positive cycle. Therefore, PDs also distribute in the position where the voltage value is zero.

PDs occurring in different discharge channels are concentrated in different positive half-cycle phases. In the initiation stage of electrical treeing, a deeper-colored ''multi-stem'' shape presents in the positive part of the pattern due to fewer electrical tree branches. With the increased applied voltage time, the number of ''stem'' increases, and the ''multi-stem'' gradually turns into a triangle due to the number of discharge channels increasing.

It can be observed from the PD patterns that the PD amplitude increases at first. Due to the existence of the space charge electric field generated by previous PD, PDs occur

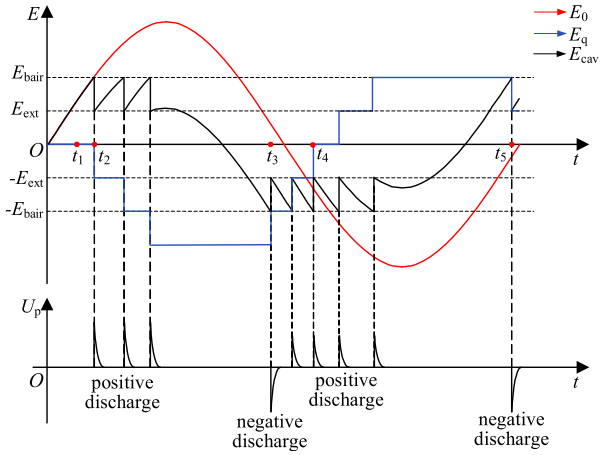

FIGURE 7. Schematic diagram of air-gap discharge in tree channels.

in a larger instantaneous voltage, so the discharge amplitude is higher. Impact ionization occurs frequently during the discharge process, resulting in the formation of the electron avalanche. The collision of the electron avalanche on the insulating material promotes the growth of the electrical trees, as shown in Figure 6(b).

It can be found that the amplitude and numbers of PD decrease after a period of compression. This may be associated with the space charge generated by previous PD, which forms a space charge shielding layer and suppresses PDs. Besides, gases produced by PD increase the air pressure in the branch channel and have an inhibitory effect on PD. However, with the increased applied voltage time, the conductivity of the channel wall increases. When it becomes a conductor, it can be assumed that the needle electrode moves forward, reducing equivalent electrode spacing. Therefore, the electric field intensity increases rapidly, resulting in intense PD in the channel, with the PD amplitude increasing and the discharge channel extending rapidly.

C. PD ENERGY

Discharge energy, W, has been considered to be greatly related to the damage degree and the life of insulating material [20]. It can be expressed by [21]:

$$W = \sum q_i n_i U_i \tag{3}$$

where q_i is the apparent charge of the ith pane, n_i is PD numbers of the ith pane, and U_i is the instantaneous value of the applied voltage of the ith pane.

Figure 8 shows the variation of electrical trees' length and PD energy in 5s with the applied voltage time in different growth modes. It can be observed that the variation of PD energy in the two half cycles is nearly the same, and the value is almost equal. This is because the PD of the electrical tree is a typical internal discharge, and its positive and negative half-cycle discharge is symmetrical. As shown in Figure 8(b), PD energy increases rapidly in the initiation stage of breakdown mode, and the electronic avalanche develops

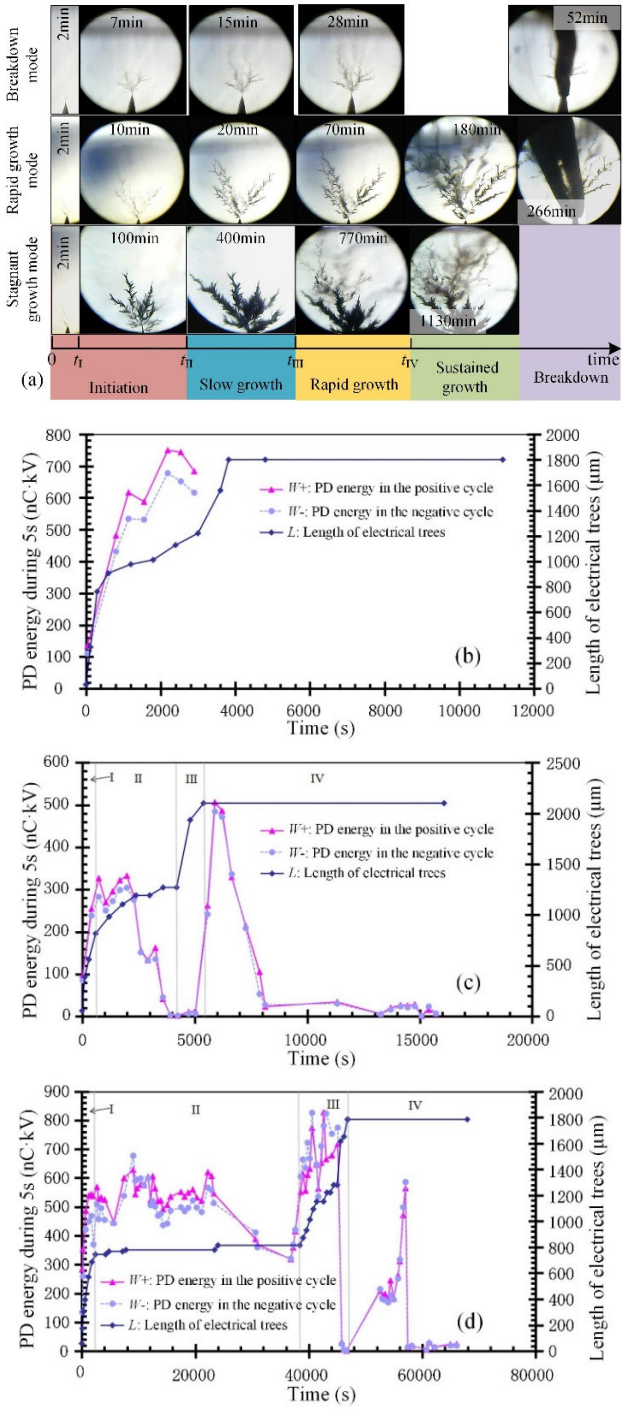

FIGURE 8. Typical growth characteristics of electrical trees: (a) the variation of electrical trees, (b) the breakdown mode, (c) the rapid growth mode, and (d) the stagnant growth mode.

quickly, leading to the rapid growth of branches. After that, the shielding effect of space charges inhibits the development of PD, resulting in a slight decrease in the growth speed. However, electrical trees extend rapidly due to the high PD energy value (600∼800 nC·kV). In the breakdown stage, PD was not measured to prevent damage to the test instrument caused by the breakdown.

Figure 8(b) shows the changes in electrical tree length and PD energy in rapid growth mode. In stage I, the PD energy increases rapidly, and the electrical tree branches grow rapidly. In stage II, PD energy decreases to zero, and the growth of electrical trees is stagnant. In stage III, PD energy increases to a maximum value (500 nC kV) in a short time, and branches propagate rapidly and reach the ground electrode. In stage IV, after electrical trees connect the insulation between the needle and plane electrodes, PD energy is reduced to 10 nC·kV. After that, PD energy fluctuates between 0 and 20 nC·kV.

Figure 8(d) shows the changes in electrical tree length and PD energy in stagnant growth mode. The variation trend is similar to that in rapid growth mode in general. Nevertheless, in stage II, the stagnation time is longer than that in fast growth mode, during which the PD energy is still high, resulting in a generation of side branches around the trunk and the electrical trees' discharge channel widening and color deepening. In stage IV, after electrical trees reach the ground electrode, PD energy increases in the applied voltage duration of 750 ∼ 950 min, leading to many new long branches adjacent to the main branches.

Analyzing the growth characteristic curves of electrical trees in different growth modes, it can be concluded that the increase of PD energy promotes the growth of electrical trees. The PD during treeing is affected by many factors such as external electric field, space-charge field, the conductivity of air-gap wall and pressure, etc [22]. The change tendency of PD energy during treeing in different samples is different even in the same experimental condition. This may be because samples are taken from the insulation of the actual cable, whose microstructure differs from other parts. So, samples are damaged by PD at different degrees after applying voltage [23], [24], resulting in the conductivity in the discharge channel wall being different and affecting the development of PD in the electrical tree growth process [25]. In the breakdown mode, the conductivity of the discharge channel wall is high, and it can be assumed that the needle electrode is moving forward and the equivalent electrode spacing decreases gradually with the growth of the electrical trees. Therefore, the electric field of the branches' tip is always high, and the PD energy always keeps a higher value, leading to the rapid insulation breakdown between the two electrodes. Suppose the conductivity of the discharge wall is small after tree initiation. In that case, the electric field of the branches' tip will decrease with the growth of electrical trees (Because the front of the branches moves forward gradually). In addition, space charges produced by previous PD have an inhibition effect on the following PD. So, the PD energy decreases, as shown in stage II of Figure 8(c).

PD extinction field strength in the air gap is proportional to the pressure, P, and the calculated formula is as follows [26]:

$$E_{ext}(t) = \frac{E_{ext0}}{p_0} P(t) \tag{4}$$

where E_{ext0} and $E_{ext}(t)$ are the initial electric field and the extinction electric field at t moment, respectively, and the P_0 and $P(t)$ are the pressure of initial moments and t moments, respectively.

In stage III of Figure 8(c), sustained PDs release much heat, and thermo-oxidative aging occurs in the material, accompanied by the fracture of the molecular chain and the generation of gases, such as H_2, CO, and CO_2. As a result, pressure in the discharge channel increases, and PDs are suppressed. However, the high-pressure stress on the air gap wall promotes the growth of electrical trees. So, the "Electrical trees extending without PD" phenomenon appears.

IV. GROWTH STAGE RECOGNITION OF ELECTRICAL TREES

PD pattern recognition can quickly and effectively identify the discharge type, providing a diagnostic basis for PD online monitoring. In this chapter, the growth stage of electrical trees with a rapid growth mode, namely the initiation (stage I), the slow growth stage (stage II), the rapid growth stage (stage III), and the sustained growth stage (stage IV), is recognized by the sparse representation as an example. Figure 9 is the block diagram of the growth stage recognition of electrical trees, which contains the data acquisition and preprocessing, building the over-complete atomic dictionary, and the growth stage recognition.

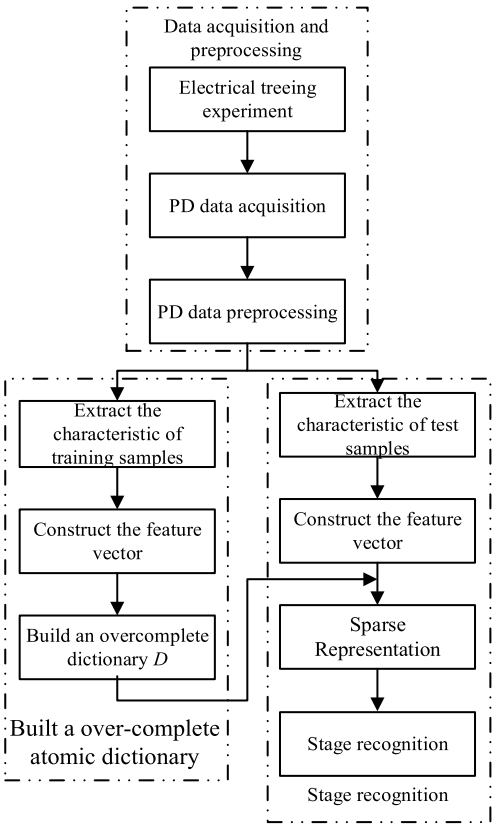

FIGURE 9. Block diagram of the growth stage recognition of electrical trees.

A. DATA ACQUISITION AND PREPROCESSING

The data in this paper is the PD of electrical trees in the rapid growth mode, which includes 100 × 4 sets of training samples and 100 × 4 sets of test samples, namely 100 sets of training samples and 100 sets of test samples in each growth stage of the rapid growth mode. Each set of samples is the PD data for 2 s, which is preprocessed to obtain the PD amplitude and phase, the number of PD pulse $H_n(\varphi)$, the maximum of PD amplitude $H_q\max(\varphi)$, and the average PD amplitude $H_q\text{avg}(\varphi)$. Figure 10 shows the typical electrical tree PD patterns in stages I and II.

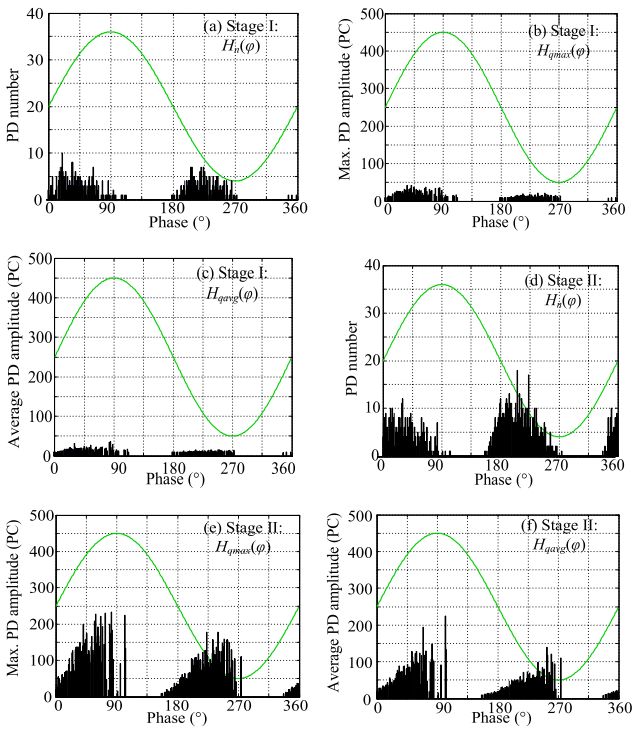

FIGURE 10. Typical PD patterns of electrical trees.

B. BUILDING THE OVER-COMPLETE ATOMIC DICTIONARY

Suppose that the sample is from space $\mathbf{R}^M$; thus, all the samples are concatenated to form a matrix, denoted as $D \in \mathbf{R}^M \times N$. When the number of the samples is larger than the dimension of samples in D, i.e., $N > M$, dictionary D is referred to as an over-complete dictionary. A signal denoted as a vector $\mathbf{x} \in \mathbf{R}^N \times 1$ can be expressed as

$$x = Ds \tag{5}$$

where $\mathbf{s} \in \mathbf{R}^M \times 1$ is the column vector of weighting coefficients.

According to equation 5, the sparse decomposition of a PD signal needs to select the fewest atoms in the established over-complete atomic dictionary to express the signal according to its characteristics effectively.

In this paper, the skewness S_k, kurtosis K_u, 1-norm $||x||_1$, 2-norm $||x||_2$, ∞-norm $||x||_\infty$ of PD patterns (*i. e.* $H_n(\varphi)$, $H_q\max(\varphi)$, and $H_q\text{avg}(\varphi)$) are characteristics to build feature vector.

The skewness S_k and kurtosis K_u are

$$S_\text{k} = \frac{\sum_{i=1}^{180}(x_i - \mu)^3 p_i}{\sigma^3} \tag{6}$$

$$K_\text{u} = \frac{\sum_{i=1}^{180}(\phi_i - \mu)^4 \cdot p_i}{\sigma^4} - 3 \tag{7}$$

where x is the vertical axis of PD patterns at the phase φ, and

$$p_i = \phi_i \Big/ \sum_{i=1}^{180}\phi_i \tag{8}$$

$$\mu = \sum_{i=1}^{180}(\phi_i \cdot p_i) \tag{9}$$

$$\sigma = \sqrt{\sum_{i=1}^{180} p_i(\phi_i - \mu)^2} \tag{10}$$

The 1-norm $||x||_1$, 2-norm $||x||_2$, ∞-norm $||x||_\infty$ are

$$\|x\|_1 = \sum_{0}^{359}\left|x^i\right| \tag{11}$$

$$\|x\|_2 = \left[\sum_{0}^{359}\left(x^i\right)^2\right]^{1/2} \tag{12}$$

$$\|x\|_\infty = \max_i \left|x^i\right| \tag{13}$$

It should be noted that the positive-cycle phase of PD pattern is taken as $-46°\sim134°$ because PD pulses in the positive cycle are not among $0°\sim179°$ as shown in Figure 10. Similarly, the negative-cycle phase of PD pattern is taken as $135°\sim314°$. The skewness S_k and kurtosis K_u in the positive and negative cycle are calculated and denoted as S_k^+, S_k^-, K_u^+, and K_u^-, respectively. Table 1 shows the characteristics of PD patterns.

TABLE 1. Partial discharge characteristic quantities.

PD pattern	S_K^+	K_u^+	S_k^-	K_u^-	$\|\|x\|\|_1$	$\|\|x\|\|_2$	$\|\|x\|\|_\infty$
$H_n(\varphi)$	f_1	f_2	f_3	f_4	f_5	f_6	f_7
$H_{qmax}(\varphi)$	f_8	f_9	f_{10}	f_{11}	f_{12}	f_{13}	f_{14}
$H_{qavg}(\varphi)$	f_{15}	f_{16}	f_{17}	f_{18}	f_{19}	f_{20}	f_{21}

The feature vector $\mathbf{F}_i^j$ is

$$F_i^j = \lambda_i^j[f_1^{i,j}, f_2^{i,j}, \cdots, f_k^{i,j}, \cdots, f_{21}^{i,j}] \tag{14}$$

where λ_i^j is the normalized coefficient, $f_k^{i,j}$ is the k-th characteristics of the j-th set of sample in stage i, *i.e.* k is 21, j is 100, and i is 4.

The over-complete atomic dictionary D can be built in accordance with the $\mathbf{F}_i^j$, (15), as shown at the top of the page.

$$D=\overbrace{\begin{bmatrix} f_1^{1,1} & f_1^{1,2} & \cdots & f_1^{1,100} \\ f_2^{1,1} & f_2^{1,2} & \cdots & f_2^{1,100} \\ \vdots & \vdots & \ddots & \vdots \\ f_{21}^{1,1} & f_{21}^{1,2} & \cdots & f_{21}^{1,100} \end{bmatrix}}^{\text{Initiation stage}} \overbrace{\begin{matrix} \cdots \\ \cdots \\ \cdots \\ \cdots \end{matrix}}^{\text{Slow growth stage}} \overbrace{\begin{matrix} \cdots \\ \cdots \\ \cdots \\ \cdots \end{matrix}}^{\text{Repid growth stage}} \overbrace{\begin{bmatrix} f_1^{4,1} & \cdots & f_1^{4,100} \\ f_2^{4,1} & \cdots & f_2^{4,100} \\ \vdots & \ddots & \vdots \\ f_{21}^{4,1} & \cdots & f_{21}^{4,100} \end{bmatrix}}^{\text{Sustained growth stage}} \tag{15}$$

C. GROWTH STAGE RECOGNITION

The matching pursuit algorithm is used to obtain the sparse solution of the test samples in the overcomplete atomic dictionary. The steps are as follows:

(1) Suppose that the number of iterations n is 1, and sparse coefficients vector $\mathbf{A}^1 = [0, 0, \ldots, 0]^{\mathrm{T}} \in \mathbf{R}^{100\times 1}$. Compute the representation residual $\mathbf{r}^n$

$$\boldsymbol{r}^{\mathrm{n}} = \mathbf{x} - DA^{\mathrm{n}} \tag{16}$$

(2) Compute the absolute value of the inner product of the representation residual $\mathbf{r}^n$ and each atom in the overcomplete atomic dictionary. The best matching atom can obtain the maximum absolute value of the inner product. The position of the best-matching atom is

$$i_n = \arg\max_i | < \mathbf{r}^n, d_i > |, i = 1,\ 2,\ \ldots\ ,\ 100 \tag{17}$$

(3) Take the elements in the line i_{n}-th of $\mathbf{A}^{\mathrm{n}}$ as $< r^n, d_{i_n} >$ and denote as $\mathbf{A}^{n+}1$

(4) Update the representation residual $\mathbf{r}^n$ using $n = n + 1$. If the representation residual satisfies

$$||r^{n+1}||_2^2 = ||x - DA^{n+1}||_2^2 \leq \varepsilon \tag{18}$$

is lower than ε, which is a very small constant, such as 0.00001 in this paper, d_i is the best-matching atom.

(5) When $i \in [1, 25]$, the PD of electrical trees represents the initiation stage; when $i \in [26, 50]$, the PD represents the slow growth stage; when $i \in [56, 75]$, the PD represents the rapid growth stage; when $i \in [76, 100]$, the PD represents the sustained growth stage.

Table 2 is the recognition result of the growth stage of electrical trees. The recognition accuracy, the ratio of total correct instances to the total instances, is 90%. The precision is the ratio of true positive predictions to the total number of positive predictions. The recognition precision is higher than 91% for stage III and stage IV.

TABLE 2. Partial discharge recognition results.

Growth stage	Stage I	Stage II	Stage III	Stage IV	Precision	Accuracy
I	87	6	4	3	87%	90%
II	5	89	3	3	89%	
III	4	2	93	1	93%	
IV	4	3	2	91	91%	

V. CONCLUSION

In this study, the relationship between PD characteristics and growth models of electrical trees was investigated by experiments. The growth stage of electrical trees was recognized based on the sparse representation. PDs of electrical treeing are mainly distributed at the rising part of sinusoidal voltage. After PD occurs, space charges accumulate on the channel wall and form the space charge electric field. The superposition of the space charge electric field and applied electric field determines the occurrence of subsequent PD. PD energy shows stage change trends in the growth process of electrical trees. Because of the gases produced by the PD, the pressure in electrical trees increases, which inhibits subsequent PD. However, the high-pressure stress promotes the growth of electrical trees. So, the "Electrical trees extending without PD" phenomenon appears. The sparse representation obtains an accuracy of 91% to recognize the growth stage of electrical trees using PD data, which provides an effective method for the defect recognition of XLPE cables.

REFERENCES

[1] X. Tao and Y. Shang, "Power supply technology of safety and high efficiency fully-mechanized coal mining technology working face of modernized mine," *J. China Coal Soc.*, vol. 35, no. 11, pp. 1930–1934, Nov. 2012.

[2] D. W. Kitchin and O. S. Pratt, "Treeing in polyethylene as a prelude to breakdown," *Trans. Amer. Inst. Electr. Eng. III, Power App. Syst.*, vol. 77, no. 3, pp. 180–185, Apr. 1958.

[3] Y. Saito, M. Fukuzawa, and H. Nakamura, "On the mechanism of tree initiation," *IEEE Trans. Electr. Insul.*, vol. EI-12, no. 1, pp. 31–34, Feb. 1977.

[4] L. A. Dissado, "Understanding electrical trees in solids: From experiment to theory," *IEEE Trans. Dielectr. Electr. Insul.*, vol. 9, no. 4, pp. 483–497, Aug. 2002.

[5] M. Bao, X. Yin, and J. He, "Analysis of electrical tree propagation in XLPE power cable insulation," *Phys. B, Condens. Matter*, vol. 406, no. 8, pp. 1556–1560, Apr. 2011.

[6] X. Chen, Y. Xu, and X. Cao, "Nonlinear time series analysis of partial discharges in electrical trees of XLPE cable insulation samples," *IEEE Trans. Dielectr. Electr. Insul.*, vol. 21, no. 4, pp. 1455–1461, Aug. 2014.

[7] X. Zhen, G. Chen, and A. E. Davies, "The categories of electrical trees in XLPE," *Adv. Technol. Electr. Eng. Energy*, vol. 42, no. 4, pp. 21–24, Apr. 2003.

[8] B. Du, "Growth characteristics of electrical tree in epoxy resin under low temperature," *High Voltage Eng.*, vol. 42, no. 2, pp. 478–484, Feb. 2016.

[9] J. Densley, T. Kalicki, and Z. Nodolny, "Characteristics of PD pulses in electrical trees and interfaces in extruded cables," *IEEE Trans. Dielectr. Electr. Insul.*, vol. 8, no. 1, pp. 48–57, Feb. 2001.

[10] J. Yang and D. Zhang, "Partial discharge phenomena due to electrical treeing in XLPE," in *Proc. 1ST IEEE Conf. Ind. Electron. Appl.*, Singapore, May 2006, pp. 132–135.

[11] R. Vogelsang, "Detection of electrical tree propagation by PD measurements," *Eur. Trans. Electr. Power*, vol. 15, no. 3, pp. 271–284, May 2005.
[12] X. Zheng, X. Feng, and Y. Wang, "The categories of electrical trees in polymer insulation," *Insulating Mater.*, vol. 5, pp. 25–28, May 2003.
[13] R. Liao, "Experimental research on electrical treeing and PD characteristics of cross-linked polyethylene power cables," *Proc. CESS*, vol. 31, no. 28, pp. 136–143, Oct. 2011.
[14] J. Zeng, "Research on the growth dynamics of electrical trees in the insulation of XLPE cables under the needle-plane electrode," *High Voltage App.*, vol. 55, no. 2, pp. 156–163, Feb. 2019.
[15] C. Forssen and H. Edin, "Partial discharges in a cavity at variable applied frequency—Part 1: Measurements," *IEEE Trans. Dielectr. Electr. Insul.*, vol. 15, no. 6, pp. 1601–1609, Dec. 2008.
[16] Z. Lei, J. Song, M. Tian, X. Cui, C. Li, and M. Wen, "Partial discharges of cavities in ethylene propylene rubber insulation," *IEEE Trans. Dielectr. Electr. Insul.*, vol. 21, no. 4, pp. 1647–1659, Aug. 2014.
[17] J. H. Mason, "Breakdown of solid dielectrics in divergent fields," *Proc. IEE B, Radio Electron. Eng.*, vol. 102, no. 5, pp. 725–727, Sep. 1955.
[18] S. Boggs and J. Kuang, "High field effects in solid dielectrics," *IEEE Elect. Insul. Mag.*, vol. 14, no. 6, pp. 5–12, Nov. 1998.
[19] S. Li and X. Zheng, *Electrical Treeing in Polymer*. Beijing, China: China Machine Press, 2006, pp. 80–102.
[20] R. Schurch, S. M. Rowland, and R. S. Bradley, "Partial discharge energy and electrical tree volume degraded in epoxy resin," in *Proc. IEEE Conf. Electr. Insul. Dielectric Phenomena (CEIDP)*, Ann Arbor, MI, USA, Oct. 2015, pp. 820–823.
[21] C. Qiu and X. Cao, *Electrical Insulation Testing Technology*. Beijing, China: China Machine Press, 2013, pp. 32–45.
[22] L. Zhou, "Influence of partial air pressure on the growth characteristics of electrical," *High Voltage Eng.*, vol. 41, no. 8, pp. 2650–2656, Aug. 2015.
[23] T. Tanaka, "Tree initiation mechanisms," in *Proc. 3rd Int. Conf. Properties Appl. Dielectric Mater.*, 1991, pp. 18–24.
[24] Y. Zhou, X. Luo, P. Yan, X. Liang, Z. Guan, and N. Yoshimura, "Influence of morphology on tree growth in polyethylene," in *Proc. Int. Symp. Electr. Insulating Mater. (ISEIM) Asian Conf. Electr. Insulating Diagnosis (ACEID) 33rd Symp. Electr. Electron. Insulating Mater. Appl. Syst.*, 2001, pp. 194–197.
[25] X. Chen, Y. Xu, X. Cao, S. J. Dodd, and L. A. Dissado, "Effect of tree channel conductivity on electrical tree shape and breakdown in XLPE cable insulation samples," *IEEE Trans. Dielectr. Electr. Insul.*, vol. 18, no. 3, pp. 847–860, Jun. 2011.
[26] A. H. Illias, "Measurement and simulation of PDs within a spherical cavity in a solid dielectric material," Ph.D. dissertation, Tony Davies High Voltage Lab., Univ. Southampton, Southampton, U.K., 2011.

ZHUORAN YANG was born in Jiangsu, China. He received the M.S. degree in electrical engineering from Imperial College London, in 2013, and the Ph.D. degree in electrical engineering from Tianjin University, China, in 2019. Since 2019, he has been a Senior Engineer with State Grid Nanjing Power Supply Company, China. His main research interests include degradation of cable insulation material and partial discharge detection.

YUAN GAO was born in Jiangsu, China. He received the M.S. degree in electrical engineering from the Nanjing University of Science and Technology, China, in 2017. Since 2017, he has been a Senior Engineer with State Grid Nanjing Power Supply Company, China. His research interests include cable insulation material development and partial discharge detection.

JINGFANG DENG was born in Shandong, China. She received the M.E. degree in electrical engineering from Shandong University, in 2019. Since 2019, she has been involved on high-voltage cables as an Engineer with State Grid Nanjing Power Supply Company, China. Her main research interests include degradation of cable insulation material development and partial discharge detection.

LIXIANG LV was born in Jiangsu, China. He received the B.Eng. degree in electrical engineering from the Nanjing Institute of Technology, in 2012. Since 2001, he has been a Senior Engineer with State Grid Nanjing Power Supply Company, China. His research interests include detection of cable insulation failure and partial discharge.